

Correlation between ^{151}Eu Mössbauer isomer shift and Judd-Ofelt Ω_6 parameters of Nd^{3+} ions in phosphate and silicate laser glasses

S. Tanabe* and T. Hanada

Department of Materials Chemistry, Faculty of Integrated Studies, Kyoto University, Sakyo-ku, Kyoto 606-01, Japan

T. Ohyagi and N. Soga

Department of Industrial Chemistry, Faculty of Engineering, Kyoto University, Sakyo-ku, Kyoto 606-01, Japan

(Received 4 June 1993)

^{151}Eu Mössbauer effect measurements were carried out for various silicate and phosphate laser glasses doped with Eu^{3+} ions instead of Nd^{3+} , for which Judd-Ofelt Ω_t parameters are known. The isomer shift (IS) for the silicate glasses decreased with an increase in the electronegativity of the network-modifying alkali and alkaline-earth metal ions, indicating a decreased $6s$ electron density of the rare-earth R^{3+} ions, i.e., covalency of the $R\text{-O}$ chemical bond. On the other hand, in phosphate glasses the IS increased with increased electronegativity. Among three Ω_t parameters of Nd^{3+} , Ω_6 , which dominates the radiative transition probability and branching ratio of the 1.3 and 1.06 μm emissions, showed a good correlation with the IS of Eu^{3+} ions in the corresponding glasses, independent of compositions. The results were explained by the more sensitive dependence of the $\Xi(s, t)$ terms in Ω_6 on the overlap integrals of $4f$ and $5d$ orbitals of rare-earth ions, compared with that in Ω_2 , which is sensitive to the odd-parity terms of the crystal field, A_{sp} .

Rare-earth-doped laser glasses have come to be important technologically as a fiber amplifier for optical telecommunication¹ and a source of nuclear fusion.² The performance of the laser glass can be altered by controlling the radiative and nonradiative decay rates of rare-earth ions in the host. As a controlling factor of the induced emission cross section of laser glasses, the set of Judd-Ofelt Ω_t parameters ($t=2, 4, 6$) of rare-earth ions in a host becomes of particular importance, since the line strength S and branching ratio β of a transition from the $|aJ\rangle$ state to $|bJ'\rangle$ are determined with the reduced matrix elements of unit tensor operator $U^{(t)}$ by^{3,4}

$$S[aJ; bJ'] = \sum_{t=2,4,6} \Omega \langle aJ \| U^{(t)} \| bJ' \rangle^2, \quad (1)$$

$$\beta_{bJ'} = A[aJ; bJ'] / \sum_{bJ'} A[aJ; bJ'], \quad (2)$$

where A is the spontaneous emission probability, which is proportional to $S[aJ; bJ']$ and given with the emission wavelength λ by

$$A[aJ; bJ'] = \frac{64\pi^4 e^2}{3h(2J+1)\lambda^3} n \left[\frac{(n^2+2)^2}{9} \right] S[aJ; bJ']. \quad (3)$$

However, there have been few reports on the relationship between the structure and Ω_t ($t=2, 4, 6$) in glasses; only a semiempirical relation between Ω_2 and the ligand field asymmetry has been reported.^{5,6} In the case of Er^{3+} , Ω_6 is the dominating factor for the radiative transition probability of the 0.55 and 1.55 μm emissions, since

$$\langle f^{11} {}^4S_{3/2} \| U^{(2,4)} \| f^{11} {}^4I_{15/2} \rangle$$

and

$$\langle f^{11} {}^4I_{13/2} \| U^{(2,4)} \| f^{11} {}^4I_{15/2} \rangle$$

are zero or much smaller than $\langle \| U^{(6)} \| \rangle$.⁷ In a previous study⁸ we clarified that among three Ω_t parameters of Er^{3+} obtained by Judd-Ofelt analysis in glasses Ω_6 is most sensitive to the overlap integrals of $4f$ and $5d$ orbitals. This was shown by means of ^{151}Eu Mössbauer spectroscopy for the Eu-substituted glasses to obtain the isomer shift, which is a measure of the $6s$ electron density of the rare-earth ions.⁹

Neodymium-doped glasses are now again attracting great interest as a fiber amplifier in the 1.3 μm region where the minimum loss window of silica fiber exists along with that at 1.55 μm .¹ Although the quantum efficiency of the $\text{Nd}^{3+} {}^4F_{3/2}$ level is large enough in fluoride and most oxide glasses compared with the $\text{Pr}^{3+} {}^1G_4$ level¹⁰ owing to its larger energy gap of $\approx 5000 \text{ cm}^{-1}$ to lower levels, the branching ratio of the ${}^4F_{3/2} \rightarrow {}^4I_{13/2}$ transition at 1.3 μm is still lower than that of the ${}^4F_{3/2} \rightarrow {}^4I_{11/2}$ at 1.06 μm used for many applications.² From the sets of $\langle \| U^{(t)} \| \rangle$ for the radiative transitions from the ${}^4F_{3/2}$ level in Table I,¹¹ it is expected that the induced emission cross section and branching ratio of the 1.3 μm lasing transition can be raised also by enhancing the Ω_6 parameter of Nd^{3+} since $\langle f^3 {}^4F_{3/2} \| U^{(2,4)} \| f^3 {}^4I_{13/2} \rangle$ are zero. In this study the isomer shift of ^{151}Eu was obtained for Eu-substituted glasses and the relationship between Ω_6 and the isomer shift (IS) was investigated.

The glass compositions investigated in this study were silicate and phosphate laser glass¹² with various alkali and alkaline-earth metal ions as a network modifier (NWM) (see Table II). The Ω_t parameters of Nd^{3+} ions¹²

TABLE I. Sets of reduced matrix elements of transitions from the $^4F_{3/2}$ level of Nd^{3+} ions (Ref. 11).

Transition	$\langle U^{(2)} \rangle$	$\langle U^{(4)} \rangle$	$\langle U^{(6)} \rangle$	λ (μm)
$^4F_{3/2} \rightarrow ^4I_{9/2}$	0.0	0.2296	0.0563	0.89
$\rightarrow ^4I_{11/2}$	0.0	0.1423	0.4070	1.06
$\rightarrow ^4I_{13/2}$	0.0	0.0	0.2117	1.33
$\rightarrow ^4I_{15/2}$	0.0	0.0	0.0275	1.87

in these glasses are plotted in Fig. 1. It is seen that $\Omega_{4,6}$ takes larger values in phosphate than in silicate glasses and varies differently with the kind of NWM. Eu-substituted glasses with the same composition were prepared and ^{151}Eu Mössbauer effect measurements were carried out at room temperature using $^{151}\text{Sm}_2\text{O}_3$ (50 mCi) as the 21.6 keV γ -ray source. The velocity calibration was done with the spectrum of magnetic splitting of $\alpha\text{-Fe}$ by a $^{57}\text{Co}(\text{Rh})$ source of 14.4 keV γ radiation. The isomer shift was determined with respect to EuF_3 . All the spectra were analyzed by least-squares fitting of a Lorentzian curve. Since the mass, ionic radius, and crystallographic character of Eu^{3+} in oxide and fluoride are similar to those of Nd^{3+} ions, the local environment of both ions in glasses should be equivalent.

The Mössbauer spectra of some glasses are shown in Fig. 2. No peak due to Eu^{2+} is revealed around -12 mm/sec. The peak positions of Eu^{3+} vary with composition. The isomer shifts obtained are plotted in Fig. 3 as a function of the electronegativity of the network-modifying cation, x_M . For the silicate systems, the IS is larger and decreases with increasing x_M , while for the phosphate it increases with increasing x_M . For the ^{151}Eu nucleus, the IS increases with electron density at the nucleus $|\Psi(0)|^2$ and is expressed by¹³

$$\text{IS} = C(|\Psi(0)|^2 - Y), \quad (4)$$

where C is positive due to the nuclear radius ratio of excited and ground states of ^{151}Eu and Y depends on the $|\Psi(0)|^2$ of the γ -ray source or velocity standard. Since the variation of only the outer 6s orbital affects $|\Psi(0)|^2$ by chemical bonding with the ligand, the IS of $^{151}\text{Eu}^{3+}$ can be a measure of the 6s electron density of trivalent rare-

TABLE II. Glass compositions.

Silicate	
Alkaline earth	$65\text{SiO}_2 \cdot 20\text{Na}_2\text{O} \cdot 15\text{MgO}$ $65\text{SiO}_2 \cdot 20\text{Na}_2\text{O} \cdot 15\text{CaO}$ $65\text{SiO}_2 \cdot 20\text{Na}_2\text{O} \cdot 15\text{BaO}$
Alkaline	$65\text{SiO}_2 \cdot 15\text{BaO} \cdot 20\text{Li}_2\text{O}$ $65\text{SiO}_2 \cdot 15\text{BaO} \cdot 20\text{Na}_2\text{O}$ $65\text{SiO}_2 \cdot 15\text{BaO} \cdot 20\text{K}_2\text{O}$
Phosphate	
Alkaline earth	$65\text{P}_2\text{O}_5 \cdot 10\text{Al}_2\text{O}_3 \cdot 25\text{MgO}$ $65\text{P}_2\text{O}_5 \cdot 10\text{Al}_2\text{O}_3 \cdot 25\text{CaO}$ $65\text{P}_2\text{O}_5 \cdot 10\text{Al}_2\text{O}_3 \cdot 25\text{BaO}$
Alkaline	$65\text{P}_2\text{O}_5 \cdot 10\text{Al}_2\text{O}_3 \cdot 25\text{Li}_2\text{O}$ $65\text{P}_2\text{O}_5 \cdot 10\text{Al}_2\text{O}_3 \cdot 25\text{Na}_2\text{O}$ $65\text{P}_2\text{O}_5 \cdot 10\text{Al}_2\text{O}_3 \cdot 25\text{K}_2\text{O}$

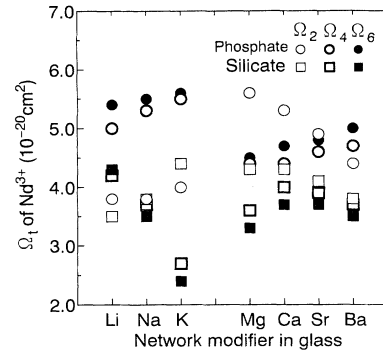


FIG. 1. Variation of Ω_r parameters of Nd^{3+} in silicate and phosphate glasses (Ref. 12).

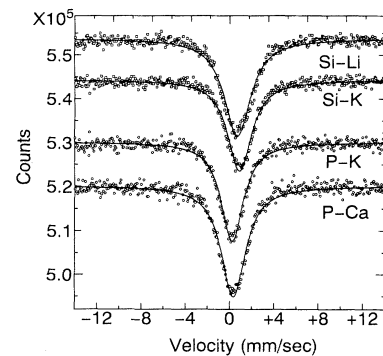


FIG. 2. ^{151}Eu Mössbauer spectra of several silicate and phosphate glasses.

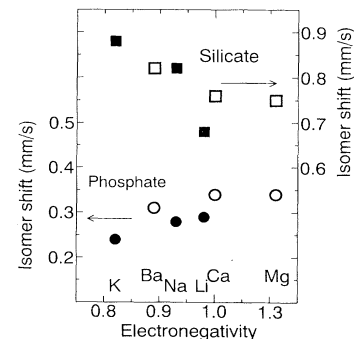


FIG. 3. Relationship between ^{151}Eu isomer shift and the electronegativity of network-modifying alkali and alkali earth in silicate and phosphate glasses.

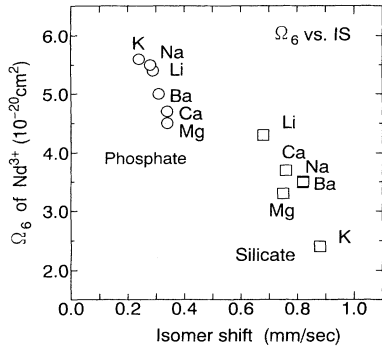


FIG. 4. Relationship between Ω_6 parameters of the Nd^{3+} and ^{151}Eu isomer shift in glasses.

earth ions in solids. The 6s electron density increases with increasing covalency of the R-O bond or the local basicity of R^{3+} sites in oxide hosts.⁹ The main contribution to the 6s orbital is from the σ electron of the 2p orbital of the oxygen ions. A much lower IS can be expected in phosphate glasses than in silicate, since the chemical bonds between the network-forming P^{5+} and oxygen are much more covalent than those in silicates, and thus the electron polarizability of oxygen is much lower. The opposite tendency of the IS against x_M in the phosphate system may be ascribed to different chain structures and oxygen polyhedra coordinating to the R^{3+} ion and also

TABLE III. Sets of integers $l, s,$ and t in Eq. (5).

l	s	t
2	1	2
(d orbital)	3	2
	3	4
	5	4
	5	6
4	5	6
(g orbital)	7	6

to the effect of delocalized π -electron donation from the resonating double bond in the P-O chains to the 5d orbital of the R^{3+} ions in glasses.

The Ω_6 parameters are plotted as a function of the IS in Fig. 4. It is to be noted that a strong correlation appears between the two parameters independent of the kind of network former. A similar situation holds for the IS and Ω_6 of Er^{3+} ions in silicate, borate, germanate, aluminate, and aluminosilicate glasses, which is shown in Fig. 5.⁸ These results can be explained as follows.

According to the theoretical expression for the intensity parameters, the values of Ω_t can be represented by⁵

$$\Omega_t = (2+1) \sum_{p,s} |A_{sp}|^2 \Xi^2(s,t) (2s+1)^{-1}, \quad (5)$$

where A_{sp} are the sets of odd-parity terms of the crystal field, and $\Xi(s,t)$ are given by³

$$\begin{aligned} \Xi_{(s,t)} &= 2 \sum_{n,l} (2f+1)(2l+1)(-1)^{f+l} \begin{Bmatrix} 1ts \\ flf \end{Bmatrix} \begin{Bmatrix} f1l \\ 000 \end{Bmatrix} \begin{Bmatrix} lsf \\ 000 \end{Bmatrix} \frac{\langle 4f|r|nl \rangle \langle nl|r^s|4f \rangle}{\Delta E(\psi)} \\ &= \sum_n \left\{ a(s,t) \frac{\langle 4f|r|nd \rangle \langle nd|r^s|4f \rangle}{\Delta E(nd)} + b(s,t) \frac{\langle 4f|r|ng \rangle \langle ng|r^s|4f \rangle}{\Delta E(ng)} \right\}, \quad (6) \end{aligned}$$

where $\Delta E(\psi)$ is the energy difference between the $4f^N$ configuration and the mixed $4f^{N-1}nl^1$ configuration, $\langle nl|r^k|n'l' \rangle$ is an abbreviation for

$$\int_0^\infty R(nl)r^k R(n'l') dr, \quad (7)$$

and R/r is the radial part of the appropriate one-electron wave function. The values $l, s,$ and t are restricted to sets of integers by the selection rules of the 3-j and 6-j sym-

bols,¹⁴ which are listed in Table III. The constants $a(s,t)$ and $b(s,t)$ in Eq. (6) are listed in Table IV. It is found that larger t takes larger s ($s=1$ or 3 for $t=2, s=3$ or 5 for $t=4,$ and $s=5$ or 7 for $t=6$). From this, Ω_6 is more greatly affected by the change of the radial integrals, $\langle 4f|r^s|nl \rangle$ than are Ω_2 and Ω_4 , and accordingly is more sensitive to the change of electron density of the 4f and the 5d orbitals, while Ω_2 is more sensitive to A_{sp} . In the case of Ω_2 , there was no systematic correlation. The radial integral $\langle 4f|r^s|5d \rangle$ decreases, as the 5d electron density decreases, and this is considered to increase with decreased 6s electron density. This is because the 6s elec-

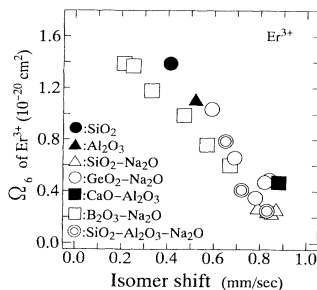


FIG. 5. Relationship between Ω_6 parameters of Er^{3+} and the isomer shift in several oxide glasses (Ref. 8).

TABLE IV. Sets of coefficients $a(s,t)$ and $b(s,t)$ in Eq. (6).

(s,t)	$a(s,t)$	$b(s,t)$
(1,2)	$-6\sqrt{14}/35$	$-2\sqrt{14}/21$
(3,2)	$8/35$	$4/7$
(3,4)	$2\sqrt{22}/21$	$2\sqrt{22}/77$
(5,4)	$-2\sqrt{70}/231$	$-4\sqrt{70}/77$
(5,6)	$-10\sqrt{14}/77$	$-10\sqrt{14}/1001$
(7,6)	0	$28\sqrt{55}/429$

trons shield or repulse the $5d$ orbital.

The tendencies observed in Figs. 4 and 5 are consistent with the idea that the change of Ω_6 is most dependent on the radial integral part, $\langle 4f|r^s|5d \rangle$ in the $\Xi(s,t)$ term because of the shielding effect of the $6s$ orbital on $5d$ electrons.

Therefore, to gain the transition probability for which Ω_6 is the most dominating factor, such as $1.33 \mu\text{m}$ for Nd^{3+} and $1.55 \mu\text{m}$ for Er^{3+} , the choice of a host with lower local basicity of rare-earth sites can be advantageous to raise the $\langle 4f|r^s|5d \rangle$ by reducing the $6s$ electron density. Systematic investigation of the rare-earth ligand field and glass structures is necessary in terms of the presence of nonbridging oxygen with higher polarizability and the linkage structure of the oxygen polyhedra.

Conclusion. The Ω_6 of Nd^{3+} ions in silicate and phos-

phate glasses are plotted versus the IS of ^{151}Eu in the same glass matrices. The Ω_6 has a good relation with the IS and becomes smaller as the IS becomes large, regardless of the kind of host compositions. This result indicates that Ω_6 is principally affected by the radial integral part $\langle 4f|r^s|nl \rangle$.

The authors would like to thank Dr. Y. Isozumi and Dr. S. Ito at Radioisotope Research Center in Kyoto University for their help in Mössbauer effect measurement. They also thank Dr. T. Izumitani and Dr. H. Toratani in HOYA Corporation for information on the Ω_i data of Nd^{3+} in laser glasses. This work was partially supported by the Grant-in-Aid for Scientific Research from the Ministry of Education, Science and Culture of Japan (No. 04553069).

*Fax: 81-75-753-6844.

¹E. Snitzer, *J. Less-Common Met.* **148**, 45 (1989).

²M. J. Weber, *J. Non-Cryst. Solids* **123**, 208 (1990).

³B. R. Judd, *Phys. Rev.* **127**, 750 (1962).

⁴J. S. Ofelt, *J. Chem. Phys.* **37**, 511 (1962).

⁵R. D. Peacock, in *Structure and Bonding*, edited by J. D. Dun-
itz *et al.* (Springer-Verlag, Berlin, 1975), Vol. 22, p. 83.

⁶S. Tanabe, T. Ohyagi, N. Soga, and T. Hanada, *Phys. Rev. B* **46**, 3305 (1992).

⁷M. J. Weber, *Phys. Rev.* **157**, 262 (1967).

⁸S. Tanabe, T. Ohyagi, S. Todoroki, T. Hanada, and N. Soga, *J. Appl. Phys.* **73**, 8451 (1993).

⁹S. Tanabe, K. Hirao, and N. Soga, *J. Non-Cryst. Solids* **113**,

178 (1989).

¹⁰Y. Ohishi and E. Snitzer, in *Proceedings of the International Conference on the Science and Technology of New Glasses, Tokyo, 1991*, edited by S. Sakka and N. Soga (Ceram. Soc., Tokyo, Japan, 1991), p. 199.

¹¹S. E. Stokowski, R. A. Saroyan, and M. J. Weber (unpublished).

¹²T. Izumitani, H. Toratani, and H. Kuroda, *J. Non-Cryst. Solids* **47**, 87 (1982).

¹³O. Berkooz, *J. Phys. Chem. Solids* **30**, 1763 (1969).

¹⁴M. Rotenberg, R. Bivens, N. Metropolis, and J. K. Wooten, *The 3-j and 6-j Symbols* (MIT Press, Cambridge, MA, 1964).